(Oxford Univ. Press, New York, 1979), pp. 75–95.
19. We thank W. Kort and J. Dortland for surgical assistance, J. Loeve for computer services, and J. V. Baker and P. Schenck for technical support; H. Koning and his staff at the TNO primate center for animal care services: J. J. van der Werff ten Bosch for support and encouragement of the project. D.A.G. was funded by a visiting scientists program of the Rotterdam Medical Faculty, and expresses appreciation to that institution. Supported in part by NIH grant RR00167.
* Present address: Wisconsin Regional Primate Research Center, 1223 Capitol Court, Madison 53706.

21 January 1980; revised 2 April 1980

Leucine Enkephalin: Localization in and Axoplasmic Transport by Sacral Parasympathetic Preganglionic Neurons

Abstract. *Nerve processes and cell bodies containing leucine enkephalin were demonstrated in the sacral autonomic nucleus of the cat by immunocytochemical methods. Enkephalinergic preganglionic perikarya were seen only when axonal transport was blocked either by colchicine or by ventral root ligation. Ligation of the sacral ventral roots also produced damming of enkephalin immunoreactivity proximal to the S_2 ligature. These data indicate that parasympathetic preganglionic neurons synthesize and transport enkephalin or enkephalin-like immunoreactive compounds to the periphery.*

In the cat, the smooth musculature of the pelvic viscera receives its innervation indirectly from parasympathetic preganglionic neurons of the sacral spinal cord. The majority of these cells are located along the lateral border of the intermediate and ventral gray matter of S_2 and upper S_3 (*1–5*). In contrast, striated pelvic sphincter muscles are innervated by a column of motor neurons in the ventral horn, which extends from S_1 to upper S_2 (*3*). These neurons form the feline homolog of the motor column of Onuf (*6*). In light of previous studies that demonstrated enkephalin in the rat autonomic nervous system and our observations of enkephalin in the feline dorsal motor nucleus of the vagus (*7*), we sought to determine whether the influence of opiates on pelvic visceral reflexes (*8*) indicates an endogenous opioid preganglionic innervation. Our results indicate that sacral parasympathetic preganglionic neurons of the spinal cord synthesize the endogenous opiate receptor ligand leucine enkephalin ([Leu]enkephalin) and transport it intra-axonally to the periphery.

We used immunocytochemical techniques to identify [Leu]enkephalin in both the sacral spinal cord and sacral ventral roots. Untreated and colchicine-treated cats were perfused via the aorta sequentially with 200 ml of 0.1*M* phosphate buffer, 2 liters of 4 percent paraformaldehyde in 0.1*M* phosphate buffer or the same fixative containing 0.2 percent glutaraldehyde, and finally with 500 ml of 0.1*M* phosphate buffer. Sacral segments S_1 to S_3 and the appropriate sacral roots were dissected, dehydrated, and embedded in paraffin. Leucine enkephalin was localized on 20-μm paraffin or 50-μm Vibratome sections by the unlabeled antibody peroxidase-antiperoxidase technique (*9*) with specific antiserum to [Leu]enkephalin conjugated to keyhole limpet hemocyanin (*10*). To control for antibody specificity, adjacent sections were incubated with [Leu]enkephalin antiserum (diluted 1:1000) that had been preabsorbed with an excess of [Leu]-enkephalin [100 μg of [Leu]enkephalin (Boehringer-Mannheim) per milliliter of antiserum]. Results of all control studies were negative.

In the sacral cord of untreated animals we found no enkephalinergic cell bodies. Enkephalin-like immunoreactivity in nerve processes was most densely concentrated in the superficial dorsal horn (laminae I and II), in the intermediate gray matter, and around the central canal (Fig. 1, A and B). In the second sacral segment, enkephalin staining was more intense along the ventrolateral border of the gray matter and adjacent lateral funiculus (Fig. 1B). This area corresponds to the intermediolateral sacral autonomic nucleus (*1–3*). Thin varicose enkephalin-containing processes were scattered throughout the sacral ventral horn. The motor column of Onuf, however, contained a rich plexus of enkephalinergic processes throughout its rostral-caudal extent (S_1 to rostral S_2) (Fig. 1A). This dense pattern of enkephalin immunoreactivity in the Onuf nucleus suggests that exogenous opiates exert a direct spinal action on somatic motor neurons of the viscera.

The distribution of sacral enkephalin perikarya was studied in two cats pretreated with colchicine. Twenty micrograms of colchicine (Sigma) dissolved in 2 μl of sterile saline was injected into the spinal cord at the L_7-S_1 junction. In addition, a pledget of Gelfoam (Upjohn) saturated with colchicine (100 μg/μl) was placed directly over the dorsal surface of spinal segments S_1 to S_3. The wound was sutured with the Gelfoam in place, and the animals were killed 17 to 48 hours later.

Two groups of labeled enkephalin perikarya appeared in the intermediate gray matter of S_2 to S_3 in the colchicine-treated animals (Fig. 1C). The distribution and morphology of these cells were strikingly similar to those of the sacral parasympathetic preganglionic neurons (*1–3*) in the cat, identified either by chromatolysis or by retrogradely transported

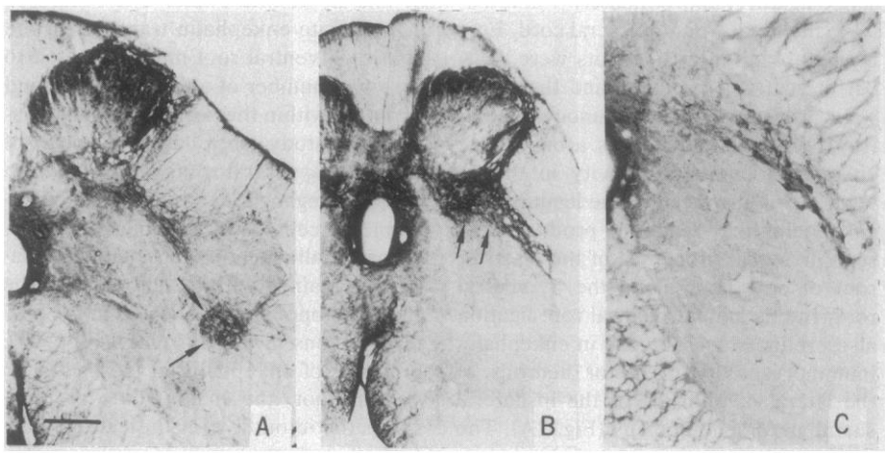

Fig. 1. Immunocytochemical localization of [Leu]enkephalin in the S_1 (A) and S_2 (B and C) sacral spinal cord of the cat. In untreated spinal cord, enkephalin-immunoreactive nerve processes are concentrated in the superficial dorsal horn, intermediate gray matter, and around the central canal. No enkephalin cell bodies are labeled. Arrows point to dense reaction product in the motor column of Onuf (A) and sacral autonomic nucleus (B). In colchicine-treated cord (C), numerous enkephalin perikarya appear in the sacral autonomic nucleus. Scale bar is 1 mm in (A) and (B) and 400 μm in (C).

0036-8075/80/0627-1479$00.50/0 Copyright © 1980 AAAS

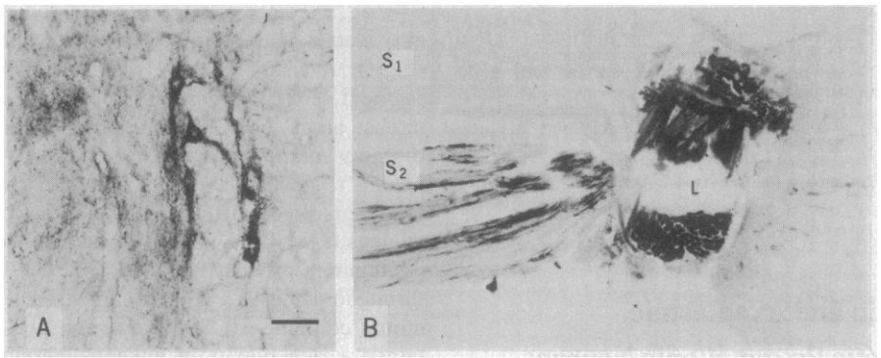

Fig. 2. Effect of ventral root ligation on [Leu]enkephalin immunoreactivity. (A) S_2 spinal cord. Enkephalin-immunoreactive perikarya are concentrated along lateral aspect of sacral autonomic nucleus (20 μm, paraffin). (B) Ligated S_1 and S_2 ventral roots. Damming of enkephalin immunoreactivity in axonal processes of S_2 ventral root is proximal to ligature (*L*) (20 μm, paraffin). Scale bar is 100 μm in (A) and 250 μm in (B).

horseradish peroxidase (HRP). One group of enkephalin somata (~ 40 by 60 μm), whose dendrites were oriented dorsoventrally, was located along the lateral gray-white border. A second group of neurons with mediolaterally oriented dendrites (~ 30 by 60 μm) was scattered throughout the intermediate gray matter, from the lateral edge of the gray matter to the central canal. No enkephalin perikarya were found in the motor column of Onuf.

To investigate whether these sacral enkephalinergic perikarya were, in fact, visceral motor neurons whose axons extend from the spinal cord, we next ligated the sacral ventral roots in untreated animals and studied the damming of enkephalin immunoreactivity at the ligature. This procedure has often been used to demonstrate axonal transport of various compounds, particularly the biogenic amines (*11*). In one animal the S_1 and S_2 ventral roots were tied together with a single ligature, approximately 4 mm distal to their exit from the sacral cord. Forty-eight hours after the roots were ligated, the cat was perfused and the tissue was processed for immunocytochemistry. Figure 2B illustrates a buildup of enkephalin immunoreactivity in the S_2 ventral root proximal to the ligature. No enkephalin-like reaction product was seen in axonal processes of the distal S_2 root or anywhere along the S_1 ventral root. In this animal, ventral root ligation also produced an increase in enkephalin immunoreactivity in motor neurons of the lateral component of the ipsilateral sacral autonomic nucleus (Fig. 2A). The average size of these labeled neurons was 22 by 50 μm. Although significantly smaller than the enkephalin perikarya seen in the intermediolateral horn after colchicine treatment, these dimensions are consistent with those of sacral autonomic neurons labeled by HRP (*1*). Apparently, colchicine produces an artifactual swelling of neuronal perikarya. No other cell body labeling was observed in the sacral cord after ventral root ligation; this includes the medial enkephalinergic, presumed parasympathetic preganglionic, neurons that were labeled after colchicine administration. Ligation of the S_3 ventral root produced no signs of enkephalin transport.

To establish that the enkephalin immunoreactivity at the ligature derived from axonal transport from the soma and not from local uptake at the ligature, the S_1 to S_3 ventral roots and S_1 to S_2 dorsal roots were individually tied with two ligatures, approximately 2 cm apart. Twenty-four hours after ligation, orthograde axonal transport of enkephalin was again blocked in the S_2 ventral root; in this case the buildup was significant only central to the most proximal ligature. Enkephalin immunoreactivity was absent in the ligated dorsal roots and in the S_1 and S_3 ventral roots. The failure to demonstrate enkephalin transport in the ligated S_3 ventral root may be related to the small number of animals studied and variation within these animals; in a physiological study of a larger number of cats, the S_3 ventral roots were shown to contain preganglionic axons in a considerable percentage of the animals (*4*).

Our results demonstrate that enkephalin is contained within cell bodies of the sacral autonomic nucleus and in their efferent axons in the S_2 ventral root. The presence of enkephalin in the ligated S_2 ventral root, the major route of parasympathetic outflow in the cat (*2*), confirms that visceral motor neurons synthesize enkephalin in the sacral autonomic nucleus. Enkephalin cell body labeling after ventral root ligation however, was confined to the intermediolateral autonomic column. The fact that a medial group of perikarya were enkephalin-immunoreactive after colchicine but not after root ligation suggests that these enkephalin neurons may differ from the medial parasympathetic motor group labeled by retrograde transport of HRP from the pelvic nerve. Alternatively, this medial enkephalin cell group may contain autonomic neurons with local arborizations that provide additional routes for enkephalin transport.

It was previously demonstrated that enkephalin is widely distributed in the autonomic nervous system (*7*). The role of enkephalin in autonomic ganglion transmission is, however, far from clear. Our demonstration of enkephalin in the S_2 ventral root and its presence in both the vagus and splanchnic nerves (*12*) indicate that the peptide is transported and stored in preganglionic nerve terminals. Since preganglionic neurons contain acetylcholine, and since a large population also contains enkephalin, these data strongly suggest that parasympathetic preganglionic nerve terminals store and perhaps release both acetylcholine and enkephalin. This arrangement would be analogous to the coexistence of biogenic amines and peptides in some central and peripheral neuron populations (*13*).

ELLYN J. GLAZER
ALLAN I. BASBAUM
Department of Anatomy, University of California, San Francisco 94143

References and Notes

1. W. C. DeGroat, I. Nadelhaft, C. Morgan, T. Schauble, *Neurosci. Lett.* **10**, 103 (1978).
2. J. E. Oliver, Jr., W. E. Bradley, T. F. Fletcher, *J. Comp. Neurol.* **137**, 321 (1969); J. M. Petras and J. F. Cummings, *Brain Res.* **153**, 363 (1978).
3. M. Sato, N. Mizuno, A. Konishi, *Brain Res.* **140**, 149 (1978).
4. W. C. DeGroat and R. W. Ryall, *J. Physiol. (London)* **196**, 563 (1968).
5. H. N. Schintzlein, H. H. Hoffman, D. M. Hamlett, E. M. Howell, *J. Comp. Neurol.* **120**, 477 (1963).
6. B. Onuf, *Arch. Neurol. Psychopathol.* **3**, 387 (1902).
7. R. Elde, T. Hokfelt, O. Johansson, L. Terenius, *Neuroscience* **1**, 349 (1979); E. J. Glazer and A. I. Basbaum, *Anat. Rec.* **193**, 549 (1979); R. I. Linnoila, R. P. DiAugustine, R. J. Miller, K. J. Chang, P. Cuatrecasas, *Neuroscience* **3**, 1187 (1978); M. Sar, W. E. Stumpf, R. J. Miller, K. Chang, P. Cuatrecasas, *J. Comp. Neurol.* **182**, 17 (1978); M. Schultzberg, T. Hokfelt, L. Terenius, L. G. Elfvin, J. M. Lundberg, J. Brandt, R. P. Elde, J. M. Goldstein, *Neuroscience* **4**, 249 (1979); M. Schultzberg, J. M. Lundberg, T. Hokfelt, L. Terenius, J. Brandt, R. P. Elde, M. Goldstein, *ibid.* **3**, 1169 (1978); G. R. Uhl, R. R. Goodman, M. J. Kuhar, S. R. Childers, S. H. Snyder, *Brain Res.* **166**, 75 (1979).
8. J. H. Jaffe and W. R. Martin, in *The Pharmacological Basis of Therapeutics*, L. Goodman and A. Gilman, Eds. (Macmillan, New York, 1975), pp. 245-283.
9. L. Sternberger, *Immunocytochemistry* (Wiley, New York, 1979).
10. Antiserum to [Leu]enkephalin conjugated to keyhole limpet hemocyanin was generously provided by S. Childers and S. Snyder, Department of Pharmacology, Johns Hopkins University.
11. A. Dahlstrom and K. Fuxe, *Z. Zellforsch. Mikrosk. Anat.* **62**, 602 (1964); A. Dahlstrom, *J. Anat.* **9**, 677 (1965).
12. J. M. Lundberg, T. Hokfelt, G. Nilsson, L. Terenius, J. Rehfeld, R. Elde, S. Said, *Acta Physiol. Scand.* **104**, 499 (1978).

13. V. Chan-Palay, G. Jonsson, S. L. Palay, *Proc. Natl. Acad. Sci. U.S.A.* **75**, 1582 (1978); T. Hokfelt, L. G. Elfvin, R. Elde, M. Schultzberg, M. Goldstein, R. Luft, *ibid.* **74**, 3587 (1977); T. Hokfelt, A. Ljungdahl, H. Steinbusch, A. Verhofstad, G. Nilsson, E. Brodin, B. Pernow, M. Goldstein, *Neuroscience* **3**, 517 (1978).
14. We thank H. J. Ralston for reviewing this paper and E. Calaustro, G. Thoren, and D. Akers for preparing histological and photographic material. This work was supported by grants NS 14627, NSF BNS78-24762, DA 01949, and research career development award NS 00364 to A.I.B. A.I.B. is a Sloan Foundation Fellow.

13 November 1979; revised 21 December 1979

Swim Bladder Volume Maintenance Related to Initial Oceanic Migratory Depth in Silver-Phase *Anguilla rostrata*

Abstract. *Gas deposition rates in the swim bladders of postmetamorphic (silver)* Anguilla rostrata *eels are about five times greater than those of premetamorphic (yellow) individuals. This extends the maximum depth at which silver eels can maintain swim bladder volume and prepares them for their spawning migration to the Sargasso Sea.*

The migration of the American eel *Anguilla rostrata* from shallow freshwater and estuarine environments to its spawning ground in the southern Sargasso Sea may occur at depths exceeding 2000 m (*1*). Before its migration offshore, *A. rostrata* undergoes a metamorphosis in which there are alterations in integument pigmentation (*2*), the visual sensory system (*3*), and the swim bladder (*4, 5*). Of these, the transformations in swim bladder morphology are most clearly related to the pronounced increase in depth during migration. The swim bladder retia mirabilia capillaries undergo a 2- to 3-fold increase in length and a 1.5-fold increase in luminal diameter, enhancing their calculated countercurrent exchange efficiency by over 300 percent (*4*). A 1.5-fold increase in the crystalline guanine content of the swim bladder wall reduces diffusive gas loss from the swim bladder by at least 15 percent (*5*). Even with this reduction, diffusive gas loss increases with depth because of the increase in the partial-pressure gradient of gas across the swim bladder wall. This volume must be replaced in order to maintain the energetic advantage for horizontal swimming imparted by neutral buoyancy (*6*).

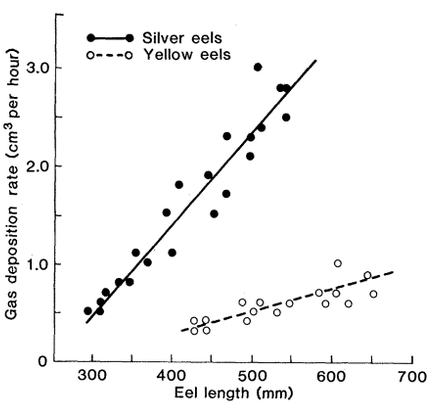

Fig. 1. Rate of swim bladder gas deposition compared with length of yellow and silver eels. Linear regression equations for the plotted lines are as follows: for yellow eels, $y = -0.7370 + 0.00246x$ ($r = .847$); for silver eels, $y = -2.3781 + 0.00942x$ ($r = .957$).

I measured gas deposition rates in yellow (premetamorphic) and silver (postmetamorphic) eel swim bladders and calculated the maximum depths at which their volume can be maintained. Eighteen yellow eels and 22 migrating silver eels, trapped in fresh and brackish water in Rhode Island during the fall of 1978, were gradually adapted to seawater and kept for 2 to 8 weeks before analysis. Determination of metamorphic phase was based on integument pigmentation and retial capillary length (in yellow eels < 2.5 mm; in silver eels > 4.5 mm).

Methodology included preliminary surgical procedures to evacuate gas from the swim bladder and pneumatic duct, followed by isolation of the gas-generating region from the gas-reabsorbing pneumatic duct (*7*). Evacuation stimulated the eel to initiate gas deposition. The rate of deposition was determined indirectly as the change in buoyant mass of the eel over a test period during which it was allowed to swim freely in a blacked-out 150-liter aquarium (*8*). For every cubic centimeter of gas generated, buoyant mass decreased 1.07 g (*9*).

Swim bladder gas deposition rates of silver eels average about five times those of equivalently sized yellow eels (Fig. 1). The linear relation between gas deposition rate and eel length is due to the elongated configuration of the body and swim bladder. Yellow eels less than 430 mm long were not tested because it was impossible to pass a ligature beneath their short retia mirabilia. Gas deposition rates of yellow *A. rostrata* are within the range reported for *A. anguilla* (*10*).

Swim bladder gases collected from ten silver eels immediately after the test period were analyzed (*11*) and found to contain 83 to 90 percent oxygen (mean, 86 percent), 7 to 13 percent carbon dioxide (mean, 10 percent), and 3 to 5 percent nitrogen (mean, 4 percent). The carbon dioxide fraction is slightly higher than the average value (7 percent) reported for *A. anguilla* (*12*).

The higher gas deposition rate in silver eels may result from a number of morphological and physiological transformations during metamorphosis. Gases deposited into the swim bladder are released from blood circulating through the vascular loop between the retia mirabilia and the acid secretory cells of the swim bladder parenchyma (*13*). An increase in the volume of blood flowing into this system increases the amount of gas available for deposition. Comparative measurements are not available for blood flow rates through the retia mirabilia of yellow and silver eels during gas deposition. However, the increase in luminal diameter of the retial capillaries during metamorphosis should permit an increase in total blood flow, making more gas available for deposition. Metamorphic increase in retial capillary length should contribute to maintenance of countercurrent function at higher rates of blood flow. Also, the amount of gas available for deposition can be increased by an elevation in hematocrit. In *A. anguilla*, hematocrit increases from 26.5 percent in yellow eels to 36.4 percent in silver eels (*14*). Because both species undergo nearly identical transformations during metamorphosis (*2–4, 15*), it is likely that *A. rostrata* also develops an elevated hematocrit.

The rate of diffusive gas loss by the

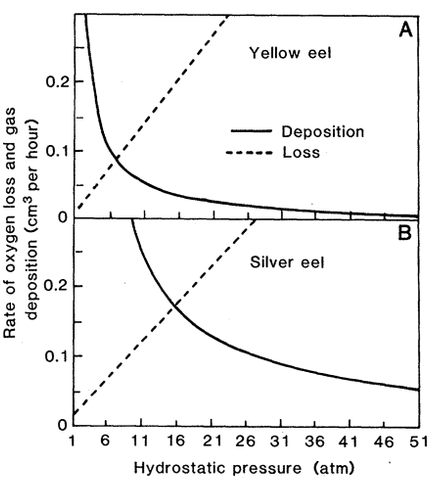

Fig. 2. Rates of swim bladder oxygen loss and gas deposition relative to hydrostatic pressure for 545-mm yellow (A) and silver (B) eels (*18*). The intersection of the two curves represents the maximum pressure at which swim bladder volume can be maintained. It is assumed that the number of moles of gas generated per unit of time remains constant with increasing depth.

0036-8075/80/0627-1481$00.50/0 Copyright © 1980 AAAS